

Chapter 2

Representation of a Stochastic Process

Numerical analysis of engineering problems in a probabilistic framework requires a representation of some stochastic processes, used for the description of the uncertainties involved in the problem. To this purpose, a continuous $mD-nV$, in the general case, stochastic process $X(t, \theta)$ needs to be represented by discrete values X_i at some discretization points $i = 1, \dots, N$. So, the main question becomes: “how can one determine the optimal approximation process (or field) $\hat{X}(\cdot)$ which will best describe the original process $X(\cdot)$ with the minimum number of random variables $\{X_i\}$?”, i.e.,

$$X(t, \theta) \approx \hat{X}(t, \theta) = \{X_i\} \quad (2.1)$$

Since, as will be shown in Chaps. 3 and 4, the computational effort in stochastic and/or reliability analysis problems is proportional to the number of random variables, the answer to this question is crucial and comes with respect to some error estimator as will be discussed later. Along these lines, all SFEM approaches are based on some kind of representation of the stochastic processes as a series of random variables. Without loss of generality this description is given for a 1D-1V stochastic process. The discretization methods can be generally categorized to the following groups:

1. **Point discretization** methods, where the random variables X_i are values of $X(t, \theta)$ at some given points t_i .

$$\hat{X}(t, \theta) = \{X_i\} = \{X(t_i, \theta)\} \quad (2.2)$$

2. **Average discretization** methods, where the random variables X_i are weighted integrals of $X(t, \theta)$ over a domain Ω_i .

$$\hat{X}(t, \theta) = \{X_i\} = \left\{ \int_{\Omega_i} X(t, \theta) c(t) d\Omega_i, \quad t \in \Omega_i \right\} \quad (2.3)$$

where $c(\cdot)$ are corresponding weights.

3. **Interpolation** methods, where the stochastic process can be approximated by interpolation at some points. Usually it is implemented in combination with some point discretization method.
4. **Series expansion** methods, where the stochastic process is represented as a truncated finite series, expressed as the decoupled product of some random variables with deterministic spatial functions. The most widely used methods of this category are the Karhunen–Loève expansion (KL) and the spectral representation (SR) methods. Both these methods belong to the family of spectral methods and $\hat{X}(t)$ is expressed as an infinite series as

$$\hat{X}(t, \theta) = \sum_{j=1}^{\infty} g_j(t) \xi_j(\theta) \quad (2.4)$$

where $\{\xi_j(\theta)\}$ are random variables considered as the coefficients of the series and $g_j(t)$ are deterministic functions over which the original field is projected.

2.1 Point Discretization Methods

The point discretization methods represent a stochastic process $\hat{X}(t, \theta)$ as discrete random variables at one or more points t_i . The value of the process at point i is then given by

$$\hat{X}(t_i, \theta) = X_i = X(t_i) \quad (2.5)$$

where t_i are the coordinates of point i . The mean value and the variance of the random variable X_i is the sample of the stochastic process at that point. The correlation between two points can be approximated from the autocorrelation function

$$R_{t_i, t_j} = R_X(t_i, t_j) \quad (2.6)$$

All the point discretization methods described next have three advantages

- The covariance matrix can be easily calculated.
- The covariance matrix is positive definite.
- The discrete random variables and the stochastic process have the same probability distribution function and for this reason the simulation process is independent of the type (pdf) of the process.

The main disadvantage of point discretization methods in the framework of stochastic finite element applications is that in order for the properties of the process to remain constant within a finite element, the size of all the elements must be small enough (fraction of the correlation length). As explained later (example 1 in Sect. 3.6), this

condition leads in certain cases to a relative dense finite element mesh which increases the computational cost.

2.1.1 Midpoint Method

The midpoint method (MP) is implemented in a discretized domain and uses the value of the stochastic process at the centroid t_i^* of the element i

$$\hat{X}(t_i, \theta) = X_i = X(t_i^*) \quad (2.7)$$

where the t_i^* coordinates are obtained from the spatial coordinates of the nodes $t_j^{(i)}$ of the element as:

$$t_i^* = \frac{1}{N} \sum_{k=1}^N t_j^{(i)} \quad (2.8)$$

where N is the number of nodes of element i . For a finite element mesh consisting of N_e elements the stochastic process $\hat{X}(t, \theta)$ is defined by the random vector $\{X_i\} = [X(t_1^*), X(t_2^*), \dots, X(t_{N_e}^*)]$.

2.1.2 Integration Point Method

The integration method can be considered as an extension of the MP method by associating a single random variable to each Gauss point of the finite element model instead of the centroid of each element. The main drawback of this method is that the total number of random variables involved increases dramatically with the size of the problem at hand.

2.1.3 Average Discretization Method

The average discretization method defines the approximated process $\hat{X}(t, \theta)$ in each finite element i as the average of the original process over the volume Ω_i of the element

$$\hat{X}(t, \theta) = X_i = \frac{1}{\Omega_i} \int_{\Omega_i} X(t, \theta) d\Omega_i, \quad t \in \Omega_i, \quad (2.9)$$

In a finite element mesh consisting of N_e elements, the approximated process $\hat{X}(t, \theta)$ is defined by the collection $\{X_i\} = [X_1, \dots, X_{N_e}]$ of these N_e random variables. The

mean and covariance matrix of $\{X_i\}$ are computed from the mean and covariance function of $X(t, \theta)$ as integrals over the domain Ω_i .

2.1.4 Interpolation Method

The interpolation method approximates the stochastic process $\hat{X}(t, \theta)$ in an element Ω_i using the values of the process at q nodal coordinates t and corresponding shape functions $N(t)$ as follows:

$$\hat{X}(t, \theta) = X_i = \sum_{j=1}^q N_j(t) X(t_j) \quad t \in \Omega_i \quad (2.10)$$

The nodal points do not necessarily coincide with the nodes of the element and the shape functions N_j can be chosen independently of the shape functions of the finite element model. The mean value and variance of the approximated field within each element are given by

$$\mathbb{E}[\hat{X}(t, \theta)] = \sum_{j=1}^q N_j(t) \mathbb{E}[X(t_j)], \quad t \in \Omega_i \quad (2.11)$$

$$\text{Var}[\hat{X}(t, \theta)] = \sum_{j=1}^q \sum_{k=1}^q N_j(t) N_k(t) R_X(t_j, t_k), \quad t \in \Omega_i \quad (2.12)$$

Each realization of $\hat{X}(\cdot)$ is a continuous function over Ω_i which is an advantage over the midpoint method. The main disadvantage of this method is that due to the interpolation, the marginal pdf of $\hat{X}(\cdot)$ is not fully consistent to the one of $X(\cdot)$.

2.2 Series Expansion Methods

2.2.1 The Karhunen–Loève Expansion

The Karhunen–Loève expansion¹ of a zero-mean random process $X(t, \theta)$ is based on the spectral decomposition of its covariance function defined as

$$C_X(t_i, t_j) = \sigma_X(t_i) \sigma_X(t_j) \boldsymbol{\rho}(t_i, t_j) \quad (2.13)$$

¹Named after the probabilist and mathematical statisticians Kari Karhunen (1907–1979) and Michel Loève (1915–1992).

where ρ is the correlation coefficient. By definition, $C_X(t_i, t_j)$ is bounded, symmetric and has the following spectral or eigen-decomposition:

$$C_X(t_i, t_j) = \sum_{n=1}^{\infty} \lambda_n \varphi_n(t_i) \varphi_n(t_j) \quad (2.14)$$

where φ_n and λ_n are orthogonal deterministic eigenfunctions and eigenvalues of the covariance function, respectively, derived from the solution of the homogeneous Fredholm integral equation of the second kind for the covariance kernel

$$\int_{\mathcal{D}} C_X(t_i, t_j) \varphi_n(t_j) dt_j = \lambda_n \varphi_n(t_i) \quad (2.15)$$

where \mathcal{D} is the domain in which the stochastic processes is defined. The key to KL expansion is to obtain the eigenvalues and eigenfunctions by solving Eq. (2.15). Because an analytical solution of Eq. (2.15) is tractable only in special cases, in general a numerical solution is the only resort.

The eigenfunctions form a complete orthogonal set satisfying the equation

$$\int_{\mathcal{D}} \varphi_k(t) \varphi_l(t) dt = \delta_{kl} \quad (2.16)$$

where δ_{kl} is the Kronecker-delta function. Any realization of $X(t, \omega)$ can thus be expanded over this basis as follows:

$$X(t, \theta) = \sum_{i=1}^{\infty} \sqrt{\lambda_n} \varphi_n(t) \xi_n(\theta), \quad t \in \mathcal{D} \quad (2.17)$$

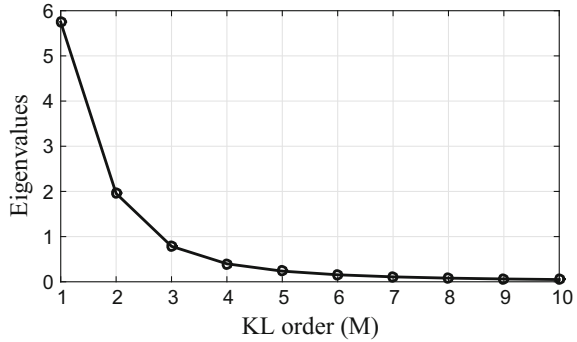
where $\xi_n(\theta)$ is a set of uncorrelated random variables with mean $\mathbb{E}[\xi_n(\theta)] = 0$ and covariance function $\mathbb{E}[\xi_k(\theta) \xi_l(\theta)] = \delta_{kl}$ which can be expressed as

$$\xi_n(\theta) = \frac{1}{\sqrt{\lambda_n}} \int_{\mathcal{D}} X(t, \theta) \varphi_n(t) dt \quad (2.18)$$

Equation (2.17) is known to converge in the mean square sense for any distribution of $X(t, \theta)$. The KL expansion of a Gaussian process has the property that $\xi_n(\theta)$ are independent standard normal variables. For practical implementation, the series is approximated by a finite number of terms M , giving

$$X(t, \theta) \approx \hat{X}(t, \theta) = \sum_{n=1}^M \sqrt{\lambda_n} \varphi_n(t) \xi_n(\theta) \quad (2.19)$$

Fig. 2.1 Decaying eigenvalues from the solution of the Fredholm integral of the second kind for $M = 10$



The corresponding covariance function is then approximated by

$$\hat{C}_X(t_i, t_j) = \sum_{n=1}^M \lambda_n \varphi_n(t_i) \varphi_n(t_j) \quad (2.20)$$

Ghanem and Spanos (1991) demonstrated that this truncated series is optimal in the mean square since the eigenvalues λ_n of Eq. (2.19) are converging fast to zero (Fig. 2.1). Thus, the choice of the covariance eigenfunction basis $\{\varphi_n(t)\}$ is optimal in the sense that the mean square error resulting from a truncation after the M -th term is minimized.

The variance error e_{var} after truncating the expansion in M terms can be easily computed as

$$e_{var} = \text{Var}[X(t, \theta) - \hat{X}(t, \theta)] = \sigma_X^2 - \sum_{n=1}^M \lambda_n \varphi_n^2(t) \quad (2.21)$$

The righthand side of the above equation means that the KL expansion always under-represents the true variance of the field.

Analytical Solution of the Integral Eigenvalue Problem

For some types of covariance functions, the Fredholm integral equation of Eq. (2.15) can be differentiated twice with respect to t_j . The resulting differential equation then can be solved analytically in order to yield the eigenvalues. An example of this class is the first-order Markov process (see Sect. 1.3.2) defined in the symmetrical domain $\mathcal{D} = [-a, a]$ and has the following covariance function:

$$C(t_i, t_j) = \sigma^2 \exp\left(-\frac{|t_i - t_j|}{b}\right) \quad (2.22)$$

where σ^2 is the variance and b is a correlation length parameter. For $\sigma = 1$ Eq. (2.15) can be written as

$$\int_{-a}^a \exp\left(\frac{|t_i - t_j|}{b}\right) \varphi_n(t_j) dt_j = \lambda_n \varphi(t_i) \quad (2.23)$$

The eigenvalues and the eigenfunctions in Eq. (2.23) can easily be estimated as follows:

- For $n = \text{odd}$,

$$\lambda_n = \frac{2b}{1 + \omega_n^2 b^2}, \quad \varphi_n(t) = c_n \cos(\omega_n t) \quad (2.24)$$

where c_n is given by

$$c_n = \frac{1}{\sqrt{a + \frac{\sin(2\omega_n a)}{2\omega_n}}}$$

and ω_n is obtained from the solution of

$$\frac{1}{b} - \omega_n \tan(\omega_n a) = 0 \quad \text{in the range} \left[(n-1)\frac{\pi}{a}, \left(n - \frac{1}{2}\right)\frac{\pi}{a}, \right] \quad (2.25)$$

- For $n \geq 2$ and $n = \text{even}$,

$$\lambda_n = \frac{2b}{1 + \omega_n^2 b^2}, \quad \varphi_n(t) = l_n \sin(\omega_n t) \quad (2.26)$$

with

$$l_n = \frac{1}{\sqrt{a - \frac{\sin(2\omega_n a)}{2\omega_n}}} \quad (2.27)$$

and ω_n being the solution of

$$\frac{1}{b} \tan(\omega_n a) + \omega_n = 0 \quad \text{in the range} \left[\left(n - \frac{1}{2}\right)\frac{\pi}{a}, n\frac{\pi}{a}, \right] \quad (2.28)$$

The solution of the Fredholm integral equation of the second kind is analytically given in the section of solved numerical examples. In this part, we need to mention that the aforementioned solutions stand for the cases of symmetrical domains \mathcal{D} . If \mathcal{D} is not symmetrical, e.g., $\mathcal{D} = [t_{\min}, t_{\max}]$, then a shift parameter $T = (t_{\min} + t_{\max})/2$ is required in order to obtain the solution and the Fredholm integral equation is solved over the domain

$$\mathcal{D}' = \mathcal{D} - T = \left[\frac{t_{\min} - t_{\max}}{2}, \frac{t_{\max} - t_{\min}}{2} \right] \quad (2.29)$$

Thus, we have

$$\hat{X}(t, \theta) = \sum_{n=1}^M \sqrt{\lambda_n} \varphi_n(t - T) \xi_n(\theta) \quad (2.30)$$

Inspection of Eq. (2.23) indicates that the quality of the simulated stochastic field is affected by the length of process relatively to the correlation parameter b and the number of KL terms M . A detailed investigation of these sensitivities was performed in Huang et al. (2001) which revealed the following important properties:

1. A low value of a/b implies a highly correlated process and hence, a relative small number of random variables are required to represent the stochastic process. Correspondingly, fewer number of terms in the KL expansion are needed for a qualitative representation.
2. The faster the autocorrelation function converges to zero, the wider is the corresponding power spectral density hence, a greater number of terms is required to sufficiently represent the underlying process by KL.
3. For a given M , the accuracy decreases as the fraction a/b increases.

For a fixed M , analytical KL gives significantly better results than numerical KL. A short description of the numerical KL is following.

Numerical Solution of the Integral Eigenvalue Problem

For random processes where the analytical solution of the Fredholm integral equation is intractable, a numerical solution is necessary. One major category of such solution schemes are the expansion methods such as the Galerkin, the collocation and the Rayleigh–Ritz methods. Galerkin methods are essentially error minimization schemes with respect to some residual calculated over the entire domain of the solution. Assuming that each eigenfunction $\varphi_n(t)$ of $C_X(t_i, t_j)$ may be represented by its expansion over a polynomial basis $\{h_i(\cdot)\}$, defined in the solution space, as

$$\varphi_n(t) = \sum_{i=1}^{\infty} d_i^n h_i(t) \quad (2.31)$$

where d_i^n are unknown coefficients to be estimated, the Galerkin procedure targets to an optimal approximation of the eigenfunctions $\varphi_n(\cdot)$ after truncating the above series in N terms and computing the residual as

$$\varepsilon_N(t) = \sum_{i=1}^N d_i^n \left[\int_{\mathcal{D}} C_X(t_i, t_j) h_i(t_j) dt_j - \lambda_j h_i(t) \right] \quad (2.32)$$

Requiring the residual to be orthogonal to the space spanned by the same basis we get

$$\langle \varepsilon_N, h_j \rangle := \int_{\mathcal{D}} \varepsilon_N(t) h_j(t) dt = 0, \quad j = 1, \dots, N \quad (2.33)$$

which leads to the following matrix eigenvalue equation:

$$\mathbf{CD} = \mathbf{ABD} \quad (2.34)$$

where

$$\mathbf{B}_{ij} = \int_{\mathcal{D}} h_i(t) h_j(t) dt \quad (2.35)$$

$$\mathbf{C}_{ij} = \int_{\mathcal{D}} \int_{\mathcal{D}} C_X(t_i, t_j) h_i(t_j) dt_j \quad (2.36)$$

$$\mathbf{D}_{ij} = d_i^j \quad (2.37)$$

$$\mathbf{A}_{ij} = \delta_{ij} \lambda_j \quad (2.38)$$

where \mathbf{C} , \mathbf{D} , \mathbf{B} and \mathbf{A} are $N \times N$ -dimensional matrices. This generalized algebraic eigenvalue problem of Eq. (2.34) can be solved for \mathbf{D} and \mathbf{A} and with backsubstitution we can estimate the eigenfunctions of the covariance kernel. This solution scheme can be implemented using piecewise polynomials for the basis $\{h_i(\cdot)\}$ of the expansion.

2.2.2 Spectral Representation Method

The spectral representation method was proposed by Shinozuka and Deodatis (1991) and generates sample functions that are ergodic in the mean value and autocorrelation. Its main property is that it expands the stochastic field to a series of trigonometric functions with random phase angles. For a zero-mean, one-dimensional stationary stochastic process $X(t, \theta)$ with autocorrelation function $R_X(t_i, t_j)$ and two-sided power spectral function $S_X(\omega)$ we can define two mutually orthogonal real-valued processes $u(\omega)$ and $v(\omega)$ with corresponding orthogonal steps $du(\omega)$ and $dv(\omega)$, respectively, such that

$$X(t, \theta) = \int_0^\infty [\cos(\omega t) du(\omega) + \sin(\omega t) dv(\omega)] \quad (2.39)$$

The processes $u(\omega)$ and $v(\omega)$ and their corresponding steps $du(\omega)$ and $dv(\omega)$, which are random variables defined for $\omega \geq 0$, satisfy the following conditions:

$$\begin{aligned} \mathbb{E}[u(\omega)] &= \mathbb{E}[v(\omega)] = 0 \quad \text{for } \omega \geq 0 \\ \mathbb{E}[u^2(\omega)] &= \mathbb{E}[v^2(\omega)] = 2S_{X_0}(\omega) \quad \text{for } \omega \geq 0 \\ \mathbb{E}[u(\omega) \cdot v(\omega')] &= 0 \quad \text{for } \omega, \omega' \geq 0 \\ \mathbb{E}[du(\omega)] &= \mathbb{E}[dv(\omega)] = 0 \quad \text{for } \omega \geq 0 \\ \mathbb{E}[du^2(\omega)] &= \mathbb{E}[dv^2(\omega)] = 2S_{X_0}(\omega) \quad \text{for } \omega \geq 0 \end{aligned} \quad (2.40)$$

$$\begin{aligned}\mathbb{E}[du(\omega)du(\omega')] &= \mathbb{E}[dv(\omega)dv(\omega')] = 0 \quad \text{for } \omega, \omega' \geq 0, \omega \neq \omega' \\ \mathbb{E}[du(\omega)dv(\omega')] &= 0 \quad \text{for } \omega, \omega' \geq 0\end{aligned}$$

In the second equation of Eq. (2.40), $S_{X_0}(\omega)$ is the differential spectral density function, whose first derivative is the spectral density function $S_X(\omega)$

$$\frac{dS_{X_0}(\omega)}{d\omega} = S_X(\omega), \quad \text{for } \omega \geq 0 \quad (2.41)$$

The inequality $\omega \neq \omega'$ in the sixth relationship of Eq. (2.40) ensures that the frequency ranges $(\omega + d\omega)$ and $(\omega' + d\omega')$ do not overlap. The spectral representation of the stationary stochastic process of Eq. (2.39) has zero-mean value and autocorrelation function equal to the target $R_X(\tau)$ since

$$\begin{aligned}\mathbb{E}[X(t, \theta)] &= \\ &= \mathbb{E}\left\{\int_0^\infty [\cos(\omega t)du(\omega) + \sin(\omega t)dv(\omega)]\right\} \\ &= \int_0^\infty \{\cos(\omega t)\mathbb{E}[du(\omega)] + \sin(\omega t)\mathbb{E}[dv(\omega)]\} \\ &= 0\end{aligned} \quad (2.42)$$

The autocorrelation function can be expressed as

$$\begin{aligned}\mathbb{E}[X(t, \theta)X(t + \tau, \theta)] &= \mathbb{E}\left\{\int_0^\infty [\cos(\omega t)du(\omega) + \sin(\omega t)dv(\omega)] \right. \\ &\quad \left. \dots \int_0^\infty [\cos(\omega' \cdot (t + \tau))du(\omega') + \sin(\omega' \cdot (t + \tau))dv(\omega')] \right\} \\ &= \int_0^\infty \int_0^\infty \cos(\omega t) \cdot \cos(\omega' (t + \tau)) \mathbb{E}[du(\omega)du(\omega')] + \\ &\quad \dots + \int_0^\infty \int_0^\infty \sin(\omega t) \cdot \sin(\omega' (t + \tau)) \mathbb{E}[du(\omega)dv(\omega')] + \\ &\quad \dots + \int_0^\infty \int_0^\infty \sin(\omega t) \cdot \cos(\omega' (t + \tau)) \mathbb{E}[dv(\omega)du(\omega')] + \\ &\quad \dots + \int_0^\infty \int_0^\infty \sin(\omega t) \cdot \sin(\omega' (t + \tau)) \mathbb{E}[dv(\omega)dv(\omega')]\end{aligned} \quad (2.43)$$

Using the last three relations of Eq. (2.40) and the above relation for $\omega = \omega'$ together with the trigonometric equality $(\cos(a - b) = \cos a \cos b + \sin a \sin b)$ we get

$$\begin{aligned}
\mathbb{E}[X(t, \theta)X(t + \tau, \theta)] &= \int_0^\infty \cos(\omega t)\cos\{\omega(t + \tau)\}2S_X(\omega)d\omega + \dots \\
&\quad + \int_0^\infty \sin(\omega t)\sin\{\omega(t + \tau)\}2S_X(\omega)d\omega + \dots \\
&= \int_0^\infty \cos(\omega\tau)2S_X(\omega)d\omega
\end{aligned}$$

Because the power spectral density function is an even function and $\sin(\omega\tau)$ an odd one, it stands that

$$2 \int_0^\infty S_X(\omega)d\omega = \int_{-\infty}^\infty S_X(\omega)d\omega \quad (2.44)$$

$$\text{and } \int_{-\infty}^\infty S_X(\omega)\sin(\omega\tau)d\omega = 0 \quad (2.45)$$

Finally we get

$$\begin{aligned}
\mathbb{E}[X(t, \theta)] &= \int_{-\infty}^\infty S_X(\omega)\cos(\omega\tau)d\omega \\
&= \int_{-\infty}^\infty S_X(\omega)e^{i\omega\tau}d\omega = \\
&= R_X(\tau)
\end{aligned} \quad (2.46)$$

Rewriting Eq. (2.39) in the following form:

$$X(t, \theta) = \sum_{k=0}^{\infty} [\cos(\omega_k t)du(\omega_k) + \sin(\omega_k t)dv(\omega_k)] \quad (2.47)$$

where $\omega_k = k \Delta\omega$ and setting $du(\omega_k)$ and $dv(\omega_k)$ as

$$\begin{aligned}
du(\omega_k) &= X_k \\
dv(\omega_k) &= Y_k
\end{aligned} \quad (2.48)$$

and if X_k and Y_k are independent random variables with zero-mean value and standard deviation equal to $\sqrt{2S_X(\omega_k)\Delta\omega}$, it can be easily proven that Eq. (2.40) is satisfied. By replacing Eq. (2.48) to (2.47) we get

$$X(t, \theta) = \sum_{k=0}^{\infty} [\cos(\omega_k t) \cdot X_k + \sin(\omega_k t)Y_k] \quad (2.49)$$

From the other hand, if we define $du(\omega_k)$ and $dv(\omega_k)$ as

$$\begin{aligned} du(\omega_k) &= \sqrt{2}A_k \cos(\Phi_k) \\ dv(\omega_k) &= -\sqrt{2}A_k \sin(\Phi_k) \end{aligned} \quad (2.50)$$

where $A_k = \sqrt{2S_X(\omega_k)\Delta\omega}$ and Φ_k are independent random phase angles uniformly distributed over the range $[0, 2\pi]$, it can be easily demonstrated that the conditions of Eq. (2.40) are satisfied. Indeed we have

$$\begin{aligned} \mathbb{E}[du(\omega_k)] &= \mathbb{E}[\sqrt{2}A_k \cos(\Phi_k)] = \\ &= \sqrt{2}A_k \int_{-\infty}^{\infty} \cos(\Phi_k) p(\Phi_k) d\Phi_k \end{aligned} \quad (2.51)$$

where $p(\Phi_k)$ is the probability density function of the random variable Φ_k with type

$$p(\Phi_k) = \begin{cases} \frac{1}{2\pi} & \text{if } 0 \leq \Phi_k \leq 2\pi \\ 0 & \text{else} \end{cases}$$

By combining the last two equations we get

$$\mathbb{E}[du(\omega_k)] = \sqrt{2}A_k \int_0^{2\pi} \frac{1}{2\pi} \cos(\Phi_k) d\Phi_k = 0 \quad (2.52)$$

In the same manner, we have $\mathbb{E}[dv(\omega_k)] = 0$. Consequently we calculate

$$\begin{aligned} \mathbb{E}[du^2(\omega_k)] &= \mathbb{E}[A_k^2 \cos^2(\Phi_k)] = \\ &= 2A_k^2 \int_0^{2\pi} \frac{1}{2\pi} (1 + \cos(\Phi_k)) \frac{1}{2\pi} d\Phi_k \\ &= 2A_k^2 \frac{1}{2\pi} = 2S_X(\omega) \end{aligned} \quad (2.53)$$

$\mathbb{E}[dv^2(\omega_k)]$ is estimated in the same way. Finally, for the random field we get

$$\begin{aligned} X(t, \theta) &= \sum_{k=0}^{\infty} [\cos(\omega_k t) \cdot \sqrt{2}(2S_X(\omega_k)\Delta\omega)^{\frac{1}{2}} \cos(\Phi_k) - \\ &\quad \dots - \sin(\omega_k t) \sqrt{2}(2S_X(\omega_k)\Delta\omega)^{\frac{1}{2}} \sin(\Phi_k)] = \\ &= \sqrt{2} \sum_{k=0}^{\infty} (2S_X(\omega_k)\Delta\omega)^{\frac{1}{2}} \cos(\omega_k t + \Phi_k) \end{aligned} \quad (2.54)$$

2.2.3 Simulation Formula for Stationary Stochastic Fields

In order to have a realization of this $X(t, \theta)$ we need to truncate the summation of Eq. (2.54) after N terms.

$$\hat{X}(t, \theta) = \sqrt{2} \sum_{n=0}^{N-1} A_n \cos(\omega_n t + \Phi_n) \quad (2.55)$$

where

$$\begin{aligned} A_n &= (2S_X(\omega_k)\Delta\omega)^{\frac{1}{2}} \quad \text{for } n = 0, 1, \dots, N-1 \\ \omega_n &= n\Delta\omega \\ \Delta\omega &= \frac{\omega_u}{N} \\ A_0 &= 0 \quad \text{or } S_X(\omega_0 = 0) = 0 \end{aligned} \quad (2.56)$$

The coefficient A_0 is chosen zero such that the temporal mean value averaged over the whole simulation time $T_0 = \frac{2\pi}{\Delta\omega}$ of the generated stochastic process $\hat{X}(t, \theta)$ remains zero in each generated sample. This is because if some power spectral contribution is added at $\omega = 0$, a random variable term is always present, shifting the temporal (sample) average apart from being zero. In order to avoid having to impose this condition the frequency shifting theorem was proposed by Zerva (1992) but with the side effect of doubling the period of the simulated field.

In Eq. (2.56) ω_u is usually applied as the uppercut off frequency after which the power spectrum becomes practically zero. In order to estimate this frequency we use the following criterion:

$$\int_0^{\omega_u} S_X(\omega) d\omega = (1 - \epsilon) \int_0^{\infty} S_X(\omega) d\omega \quad (2.57)$$

where $\epsilon \ll 1$ is the “admissible relative error”. The target autocorrelation function $R_{\hat{X}}(\tau)$ is given by

$$R_{\hat{X}}(\tau) = \int_{-\omega_u}^{\omega_u} S_X(\omega) e^{i\omega\tau} d\omega = \int_0^{\omega_u} 2S_X(\omega) \cos \omega\tau d\omega \quad (2.58)$$

The difference between these two functions

$$\epsilon^*(\tau) = R_X(\tau) - R_{\hat{X}}(\tau) = \int_{\omega_u}^{\infty} 2S_X(\omega) \cos(\omega\tau) d\omega \quad (2.59)$$

corresponds to the mean square simulation error due to the truncation of the spectral density function for $|\omega| \geq \omega_u$, which is termed “truncation error”.

One sample function of the stochastic process can be generated by replacing the phase angles $\Phi_0, \dots, \Phi_{N-1}$ in Eq. (2.55) with their corresponding sample values $\phi_0(\omega), \dots, \phi_{N-1}(\omega)$, as these can be generated by some random number generator as follows:

$$\hat{X}(t, \theta) = \sqrt{2} \sum_{n=0}^{N-1} A_n \cos(\omega_n t + \phi_n(\theta)) \quad (2.60)$$

It must be mentioned that the step Δt of the generated sample functions must satisfy the following condition in order to avoid aliasing.

$$\Delta t \leq \frac{\pi}{\omega_u} \quad (2.61)$$

The sample functions generated by Eq. (2.60) are obviously bounded by

$$|\hat{X}(t, \theta)| \leq \sqrt{2} \sum_{n=0}^{N-1} A_n \quad (2.62)$$

For the cases of 2D and 3D spectral representation, Eq. (2.60) takes the form

$$\begin{aligned} \hat{X}(t, \theta) = \hat{X}(t_1, t_2, \theta) = & \sqrt{2} \sum_{i=1}^{N_1} \sum_{j=1}^{N_2} A_{ij} [\cos(\omega_{1i} t_1 + \omega_{1j} t_2 + \phi_{ij}^1(\theta)) + \\ & + \cos(\omega_{1i} t_1 - \omega_{2j} t_2 + \phi_{ij}^2(\theta))] \end{aligned}$$

and

$$\begin{aligned} \hat{X}(t, \theta) = \hat{X}(t_1, t_2, t_3; \theta) = & \sqrt{2} \sum_{i=1}^{N_1} \sum_{j=1}^{N_2} \sum_{k=1}^{N_3} A_{ijk} [\cos(\omega_{1i} t_1 + \omega_{2j} t_2 + \omega_{3k} t_3 + \phi_{ijk}^1(\theta)) + \\ & + \cos(\omega_{1i} t_1 + \omega_{2j} t_2 - \omega_{3k} t_3 + \phi_{ijk}^2(\theta)) + \\ & + \cos(\omega_{1i} t_1 - \omega_{2j} t_2 + \omega_{3k} t_3 + \phi_{ijk}^3(\omega)) + \\ & + \cos(\omega_{1i} t_1 - \omega_{2j} t_2 - \omega_{3k} t_3 + \phi_{ijk}^4(\omega))] \end{aligned} \quad (2.63)$$

respectively, with

$$\begin{aligned} A_{ij} &= \sqrt{2S_X(\omega_1, \omega_2) \Delta\omega_1 \Delta\omega_2} \\ A_{ijk} &= \sqrt{2S_X(\omega_1, \omega_2, \omega_3) \Delta\omega_1 \Delta\omega_2 \Delta\omega_3} \end{aligned}$$

$$\Delta\omega_{1,2,3} = \frac{\omega_{(1,2,3)u}}{N_{1,2,3}}$$

$$\omega_{1,2,3} = (t_1, t_2, t_3)\Delta\omega_{1,2,3}$$

The numbers $N_{1,2}$ and $N_{1,2,3}$ of independent angle phases $\varphi(\theta)$ generated randomly in the range $[0, 2\pi]$ for the cases of two and three-dimensional random fields, respectively, are:

$$N_{1,2} = 2N_1N_2 \quad (2.64)$$

and

$$N_{1,2,3} = 4N_1N_2N_3 \quad (2.65)$$

respectively.

2.3 Non-Gaussian Stochastic Processes

In nature, most of the uncertain quantities appearing in engineering systems are non-Gaussian (e.g., material, geometric properties, seismic loads). Nevertheless, the Gaussian assumption is often used due to lack of relevant experimental data and for simplicity in the mathematical implementation. It must be noted that this assumption can be problematic in many cases. For example, in the case where the Young's modulus is assumed to be a random variable following a Gaussian distribution, negative values for the Young's modulus may occur which have no physical meaning. For this reason, the problem of simulating non-Gaussian stochastic processes and fields has received considerable attention. However, the KL and Spectral representation methods, as discussed above, are limited in generating realizations of Gaussian stochastic processes due to the central-limit theorem, since the random variables in the summation formulas are independent.

In order to fully characterize a non-Gaussian stochastic process all the joint multidimensional density functions are needed which is generally not possible. For this reason a simple transformation of some underlying Gaussian field with known second-order statistics can be used in order to simulate a non-Gaussian stochastic process. If $X(t, \theta)$ is a stationary zero-mean Gaussian process with unit variance and spectral density function (SDF) $S_X(\omega)$, a homogeneous non-Gaussian stochastic process $y(t, \theta)$ with power spectrum $S_y^T(\omega)$ can be defined as

$$y(t, \theta) = Y^{-1}\Phi[X(t, \theta)] \quad (2.66)$$

where Φ is the standard Gaussian cumulative distribution function and Y is the non-Gaussian marginal cumulative distribution function of $y(t, \theta)$. The transformation $Y^{-1}\Phi$ is a memory-less translation since the value of $y(t, \theta)$ at an arbitrary point t depends on the value of $X(t, \theta)$ at the same point only. The resulting non-Gaussian field $y(t, \theta)$ is called a translation field.

The main shortcoming of translation fields is that, although the mapped sample functions of (2.66) will have the prescribed target marginal probability distribution Y , their power spectrum will not be identical to $S_y^\top(\omega)$. Another important issue, pointed out by Grigoriu (1984), is that the choice of the marginal distribution of $y(t, \theta)$ imposes constraints to its correlation structure. In other words, Y and $S_y^\top(\omega)$ have to satisfy a specific compatibility condition derived directly from the definition of the autocorrelation function of the translation field as

$$R_y^\top(\tau) = \int_{-\infty}^{+\infty} \int_{-\infty}^{+\infty} Y^{-1}[\Phi(X_1)]Y^{-1}[\Phi(X_2)]\phi[X_1, X_2; R_X(\tau)]dX_1dX_2 \quad (2.67)$$

where $X_1 = X(t, \theta)$, $X_2 = X(t + \tau, \theta)$ and ϕ is the pdf of the underlying Gaussian field. If these two quantities are proven to be incompatible through (2.67), then no translation field can be found having the prescribed characteristics. In this case, one has to resort to translation fields that match the target marginal distribution and/or SDF approximately.

2.4 Solved Numerical Examples

1. For an 1D-1V, zero-mean, Gaussian stochastic process $X(t, \theta)$ defined in the range $[-a, a]$ and with autocorrelation function $R_X(t_i, t_j)$ given by

$$R(t_i, t_j) = \sigma^2 \exp\left(-\frac{|t_i - t_j|}{b}\right) \quad (2.68)$$

Solve the Fredholm integral equation in order to estimate the eigenvalues and the eigenfunctions of the KL expansion.

Solution:

The Fredholm integral equation of the second kind is defined as

$$\int_{-a}^{+a} \sigma^2 \exp(-c|t_i - t_j|)\varphi(t_j)dt_j = \lambda\varphi(t_i) \quad (2.69)$$

where $c = 1/b$. Equation (2.69) can be written as

$$\int_{-a}^{t_i} \sigma^2 e^{(-c|t_i - t_j|)}\varphi(t_j)dt_j + \int_{t_i}^{+a} \sigma^2 e^{(-c|t_i - t_j|)}\varphi(t_j)dt_j = \lambda\varphi(t_i) \quad (2.70)$$

Differentiating the above equation once with respect to t_i gives

$$\lambda\varphi'(t_i) = -\sigma^2 c e^{-ct_i} \int_{-a}^{t_i} e^{ct_j} \varphi(t_j)dt_j + \sigma^2 c e^{ct_i} \int_{t_i}^{+a} \sigma^2 e^{-ct_j} \varphi(t_j)dt_j \quad (2.71)$$

and differentiating a second time gives

$$\lambda\varphi''(t) = (\lambda c^2 - 2\sigma^2 c)\varphi(t) \quad (2.72)$$

If we define $\omega^2 = \frac{-\lambda c^2 + 2\sigma^2 c}{\lambda}$ then Eq. (2.72) becomes

$$\varphi''(t) + \omega^2\varphi(t) = 0 \quad (2.73)$$

Thus, the integral in Eq. (2.69) is transformed to the ordinary differential equations of Eq. (2.73) and evaluating Eqs. (2.70) and (2.71) at $t = -a$ and $t = a$ we can estimate its boundary conditions as

$$\begin{aligned} c\varphi(a) + \varphi'(a) &= 0 \\ c\varphi(-a) - \varphi'(-a) &= 0 \end{aligned} \quad (2.74)$$

Solving these equations simultaneously we get the eigenvalues and eigenfunctions described in Sect. 2.2.1.

2. Consider an 1D-1V truncated (its values are either bounded below and/or above), zero-mean Gaussian (TG) stochastic process $X(t, \theta)$, obtained from an underlying Gaussian process (denoted by $g(t, \theta)$), as follows:

$$X(t, \theta) = \begin{cases} g(t, \theta) & \text{if } |g(t, \theta)| \leq 0.9 \\ 0.9 & \text{otherwise} \end{cases}$$

Use the following two spectral density functions for the description of $g(t, \theta)$

$$\text{SDF}_1 : S_g(\omega) = \frac{1}{4}\sigma_g^2 b^3 \omega^2 e^{-b|\omega|} \quad (2.75)$$

$$\text{SDF}_2 : S_g(\omega) = \frac{1}{2\pi}\sigma_g^2 \sqrt{\pi b} \omega^2 e^{-\frac{1}{4}b\omega^2} \quad (2.76)$$

with $\sigma = 0.2$ and $b = 1$. Generate realizations of the non-Gaussian process $X(t, \theta)$ and estimate its power spectral density $S_{X_{TG}}(\omega)$.

Solution:

Spectrum SDF_1 has zero power at $\omega = 0$, while spectrum SDF_2 has its maximum value at $\omega = 0$. For both spectra, b is a correlation length parameter. Simulate the underlying Gaussian process $g(t)$ according to SDF_1 and SDF_2 using the spectral representation method and then get the truncated Gaussian process $X_{TG}(t, \theta)$ by truncating the simulated Gaussian process $g(t, \theta)$ in the following way: if $g(t, \theta) > 0.9$ set $g(t, \theta) = 0.9$ or if $g(t, \theta) < -0.9$ set $g(t, \theta) = -0.9$.

Because the simulated non-Gaussian process $X_{TG}(t, \theta)$ is obtained as a nonlinear transformation of the underlying Gaussian process $g(t, \theta)$, its spectral density

functions $S_{X_{TG}}(\omega)$ is going to be different from SDF_1 and SDF_2 . The new spectral density functions of the truncated fields can be computed by producing samples $X_{TG}(t, \theta)$ and computing the spectra from Eq. (1.28). The $S_{X_{TG}}(\omega)$ is eventually determined by ensemble averaging.

2.5 Exercises

1. For a nonstationary Wiener–Levy stochastic process with covariance function

$$C_X(t_i, t_j) = \sigma^2 \min(t_i, t_j) \quad (2.77)$$

where $0 \leq t \leq a$, the Fredholm integral equation can be solved analytically. Find the eigenvalues and eigenfunctions.

2. For an 1D-1V stationary and zero-mean Gaussian stochastic process $X(t, \theta)$ with $t \in [0, 1]$ the autocorrelation function $R_X(t_i, t_j)$ is defined as

$$R(t_i, t_j) = \sigma^2 \exp\left(\frac{|t_i - t_j|}{b}\right) \quad (2.78)$$

with σ being the standard deviation and b the correlation length parameter. Using the KL expansion:

- a. Calculate the first 10 eigenvalues and eigenfunctions by solving the Fredholm integral equation analytically and numerically, for $\sigma = b = 1$.
 - b. For $b = 1$ estimate the approximated covariance function and compare it with the exact one using $M = 2, 5, 10$ terms in the truncated KL.
 - c. Plot 1000 realizations of the approximated process and calculate its probability distribution at $t = 0.5$.
3. For the 1D-1V zero-mean Gaussian stochastic process $X(t, \theta)$ with autocorrelation function

$$R_X(\tau) = \sigma^2 \frac{b^2(b - 2\tau)}{(b + 3)} \quad (2.79)$$

where b is the correlation length parameter, σ^2 is the variance of the stochastic process and $\tau \in [0, 10]$:

- a. Generate 1000 realizations of the process for $b = 1$ and $\sigma^2 = 0.8$ using the spectral representation method.
- b. Discretize the domain in $n = 11$ points, i.e., 10 elements, and represent the stochastic field at these points using the midpoint method.

- c. Use the local average method to simulate the random variables at the same midpoints. Compare the properties of the random process with these of the midpoint method.
4. For the Gaussian stochastic process of exercise 3, simulate the 1000 realizations using the KL method for $M = 1, \dots, 6$ terms in the truncated series, and $b = 1$ and 10. Estimate the corresponding power spectrums and compare them with the exact ones.
5. Generate 1000 realizations of (a) a lognormal translation process, and (b) a triangular pdf translation process using the underlying Gaussian process with the two spectral densities functions SDF_1 , SDF_2 given in example 2 in the section of solved numerical examples and then estimate the resulting non-Gaussian Spectra.

<http://www.springer.com/978-3-319-64527-8>

Stochastic Finite Element Methods

An Introduction

Papadopoulos, V.; Giovanis, D.G.

2018, XXI, 138 p. 53 illus., 26 illus. in color., Hardcover

ISBN: 978-3-319-64527-8